Kirk-Othmer Encyclopedia of Chemical Technology.

SEPARATION, SIZE SEPARATION

Size separation, the parceling of particulate material on the basis of size, is an important industrial unit operation that produces, on a continuous basis, coarser and finer streams from a feed stream in a single stage or multiple stages. Multiple stages of size-separation devices can be arranged to produce multiple streams of differing degrees of fineness, such as various grades of aggregates or coals. Multiple staging, ie, multiple stages combined with blending, is also practiced to produce two streams, in the same manner as a single-stage separation, except more efficiently. Examples are the degritting of starch (qv) or paper (qv) pulp (qv). Size separation devices are also used in conjunction with other unit operations, such as closed-circuit crushing and grinding.

Devices for size separation fall into two general categories: those basically involving the probability of passing through an aperture and those that separate by forces of fluid dynamics. The former, probability size separation, is based on the repeated presentations of particles to uniformly sized apertures in screen decks. The latter, fluid-dynamic size separation, takes advantage of the interplay between gravity and drag forces. If the particles are conveyed in a liquid, the separation is termed wet sizing; if conveyed in a gas, the separation is termed dry sizing.

A method of presenting particle size data is as the cumulative fraction (or percentage) finer than (or coarser than) some size, termed a particle size distribution (PSD). The precise definition of particle size is, however, very difficult (1). It is usually defined on the basis of the size analysis method. Fluid-dynamic partitioning is also influenced by other particle properties such as relative density or shape, as is probability partitioning, though to a much lesser degree. Size separation implies that these properties are relatively constant among the particles, and that the size is the basis of the partitioning. If, on the other hand, there are several properties that influence the separation, then this is sorting and interpretation of the separation is not possible (see Mineral recovery and processing). In order to interpret the size separation, the particles must be grouped into subpopulations of common properties.

Screening devices are used to make coarser separations; that is, fine products having 95% passing ca 100-mm–50-μm size. Dry-screening devices have a lower recommended size of ca 500 μm. Wet-screening devices that produce 95% passing ca 500–50-μm size are continually being improved.

Fluid-dynamic separating devices, called classifiers, are used to make finer separations; that is, fine products having 95% passing ca 1000–5-μm size. However, different devices have different separating ranges. For example, hydraulic-settling classifiers based on gravity sedimentation principles produce fine streams in the range of 95% passing ca 1000–100-μm size. Hydraulic-centrifugal classifiers (hydrocyclones) based on multiple *g*-force sedimentation principles, produce fine streams in the range of 95% passing ca 500–5-μm size.

Generally, as the product size becomes finer, the capacity of the separating device decreases. Thus, there are devices that can be fed hundreds of metric tons per hour (MTPH) and produce a 95% passing 50-μm product; but a device that produces 95% passing 5 μm may have a capacity of ca 1 MTPH or less.

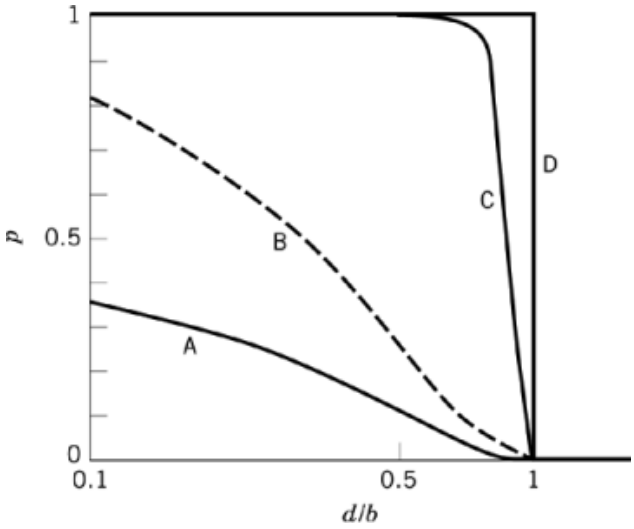

Fig. 1. Probability of a particle size d passing through a square aperture of size b. See text for discussion of the various curves.

1. Evaluation of Size Separations

Common separating devices are evaluated as follows. Consider a flat screen plate having square openings of dimension b and centers of dimension c. Ideally, the chance of a spherical particle having diameter d passing through an opening would be zero for all particles of relative size $d/b > 1$ and one for all particles of relative size $d/b < 1$. A plot of the probability-of-passing vs size (Fig. 1, curve D) is a step function, and the separation size, so-called cut size, is $d/b = 1$. A perfect separation is one where all particles of size less than the cut size pass and all particles of size greater than the cut size are retained.

However, the probability of such a particle passing, when approaching the screen plate normally, is as shown in equation 1 (2):

$$p = \left(\frac{b-d}{c}\right)^2 \qquad (1)$$

If the c/b ratio is 1.5, a typical industrial value, then the plot of the probability-of-passing equation vs size (Fig. 1, curve A) is curvilinear. If each particle that did not pass is given another opportunity, then the probability of a particle passing after n opportunities is $1 - q^n$, where q, the probability of a particle not passing, is equal to $1 - p$. The plot of probability-of-passing vs size (Fig. 1, curve C) for a very good industrial screen ($n = 100$) is an improved curve approaching the perfect separation step function. Even the curve for $n = 1000$ does not match the ideal curve; rather, it only approaches the ideal because particles of a size close to the dimension of the openings, so-called near size particles, still have a finite probability of not passing.

The characteristic curve is used to evaluate the separation because the deviation from the perfect step function represents a measure of the efficiency of the separation. A commonly used measure to characterize the shape of the curve for a size separation is the sharpness index, given the symbol κ. It is the ratio of the size of a particle having a 75% chance of passing or reporting to the finer stream, ie, d_{75}, to the size of a particle having a 25% chance of passing, ie, d_{25}. A perfect separation would give a value of 1, whereas merely a splitting action (no size separation) would give a value of 0. The sharpness index of curve C (Fig. 1) is 0.84/0.92 or 0.9. Another measure not as commonly used is the quartile deviation where one-half the absolute difference between the

upper quartile value, d_{75}, and the lower quartile value, d_{25}, is given the symbol, e_p. The quartile deviation of a perfect size separation would be 0. It is 0.04 for curve C (Fig. 1). Both of these measures represent the inefficiency of the separation.

For size separations, the equiprobable size, ie, the size of a particle that has a 50/50 chance of passing, d_{50}, is used to define the cut size. Other cut size definitions for a size separation have been used, including the 95% passing size of the fine stream, x_{95}; the size at which the cumulative fraction less than in the feed stream is equal to the yield, ie, the ratio of the fine stream flow rate to the feed stream flow rate; and the size at which the cumulative percentage less than in the fine stream is equal to the cumulative percentage greater than in the coarse stream. The d_{50} is gaining wide acceptance as the definition of cut size. The cut size for curve C is 0.9, which is less than the aperture size. This is the reason the aperture size for industrial screens is normally 10–20% larger than the desired cut size.

Curve A exhibits another characteristic: it does not go to one at d/b equal to zero (see eq. 1). This can be viewed as an apparent bypassing, or short-circuiting, of the feed material to the coarse stream, ie, a fraction of all of the particles in the feed did not pass through the screen. If the separating action of a device is viewed as a splitting action (a certain portion of the feed sent to one stream, the rest to a second, independent of size) followed by the size separation of the second stream and the blending of the coarse particles with the first stream, then the apparent bypassing represents the splitting action portion of the separation. This is a second source of inefficiency; hence, the unique value of q at d/b equal to zero is assigned the symbol a. The p values can be corrected for the apparent bypassing by dividing each value by $(1 - a)$. The corrected p values, representing the probability of a particle not split to the coarse stream passing, for curve A are shown (see Fig. 1) as curve B. The κ (0.265) and d_{50} (0.3) values must then be determined from this corrected curve, not the uncorrected one. Apparent bypassing of the feed material to the fine stream is also possible; however, such an occurrence would represent a device malfunction, eg, big holes in the screen, which is correctable. Apparent bypass cannot always be corrected, and can be present even for a corrected curve such as curve C because of the splitting action of the device. Thus a separator can have a constant corrected curve with increasing feed rate, but an increasing a value. If a size separation device is to be utilized for dedusting, ie, the production of a fine particle-free coarse stream, then obviously it should not have an apparent bypass value.

By solving the appropriate convection–diffusion equations (3) for the movement of solids in fluids, either at free-settling or hindered-settling conditions, similar characteristic curves result that increase in steepness (the sharpness index increases) and decrease in the cut size with increasing time. These curves also can have apparent bypassing to the coarse stream, but should not have apparent bypassing to the fine stream. A typical curve, a plot of the probability-of-reporting-to-the-coarse stream vs log size, is shown in Figure 2.

The characteristic separation curve can be determined for any size separation device by sampling the feed, and coarse and fine streams during steady-state operation. A protocol for determining such selectivity functions has been published (4). This type of testing, when properly conducted, provides the relationships among d_{50}, κ, and a at operating conditions. These three parameters completely describe a size separation device and can be used to predict the size distribution of the fine and coarse streams.

All three parameters, the cut size, sharpness index, and apparent bypass, are used to evaluate a size separation device because these are assumed to be independent of the feed size distribution. Other measures, usually termed efficiencies, are also used to evaluate the separation achieved by a size separation device. Because these measures are dependent on the feed size distribution, they are only useful when making comparisons for similar feeds. All measures reduce to either recovery efficiency, classification efficiency, or quantitative efficiency. Recovery efficiency is the ratio of the amount of material less than the cut size in the fine stream to the amount of material less than the cut size in the feed stream. Classification efficiency is defined as a corrected recovery efficiency, ie, the recovery efficiency minus the ratio of the amount of material greater than the cut size in the fine stream to the amount of material greater than the cut size in the feed stream. Quantitative efficiency is the ratio of the sum of the amount of material less than the cut size in the fine stream plus the amount of material greater than the cut size in the coarse stream, to the sum of the amount of material less than the cut

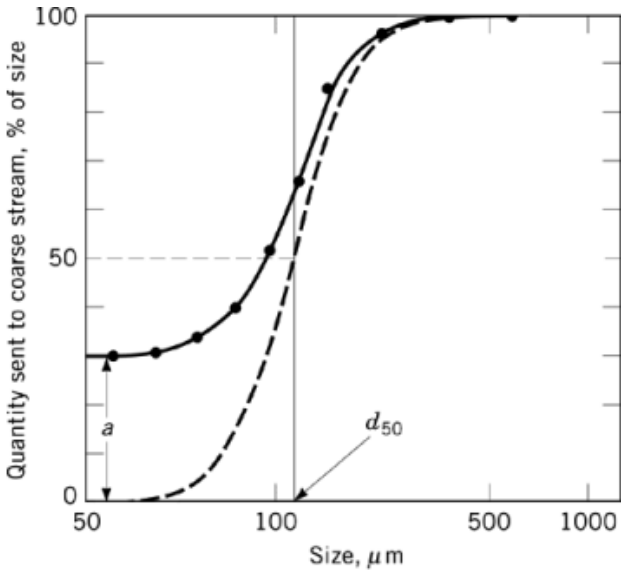

Fig. 2. Probability of a particle reporting to the coarse stream in a fluid dynamic classifier where the vertical line is the ideal classification at d_{50}; (—) is the separation curve; and (— — —), the corrected curve.

size in the feed stream plus the amount of material greater than the cut size in the feed stream. Thus, if the feed stream analyzes 50% less than the cut size and the fine stream analyzes 95% less than the cut size and the fine stream flow rate is one-half the feed stream flow rate, then the recovery efficiency is 95%, the classification efficiency is 90%, and the quantitative efficiency is 95%.

There are relationships between the independent size separation device parameters and the dependent size separation efficiencies. For example, the apparent bypass value does not affect the size distribution of the fine stream but does affect the circulation ratio, ie, the ratio of the coarse stream flow rate to the fine stream flow rate. The circulation ratio increases as the apparent bypass increases and the sharpness index decreases. Consequently, the yield, the inverse of the circulating load (the ratio of the feed stream flow rate to the fine stream flow rate or the circulation ratio plus one), decreases; hence the efficiencies decrease. For a device having a sharpness index of 1, the recovery efficiency is equal to $(1 - a)$.

There is a unique d_{50} value which produces a fine stream having a specific 95% passing size from a feed stream. The feed size distribution should analyze at least 50% less than the 95% passing size of the product (5). However, the necessary d_{50} value varies with the sharpness index value. In general, the required d_{50} decreases, as the sharpness index decreases (eq. 2):

$$d_{50} \cong (\kappa + 0.16)\, x_{95} \qquad (2)$$

This is undesirable because generally the capacity of a device is much less when operating at a lower d_{50} value.

2. Screening

Screening is a process whereby particles are presented in an appropriate manner to a series of apertures of fixed dimensions that allow finer particles to pass through into the undersize, and coarser particles to be retained in the oversize. In addition to sizing, screens are used for desliming, ie, the removal of very small particles from

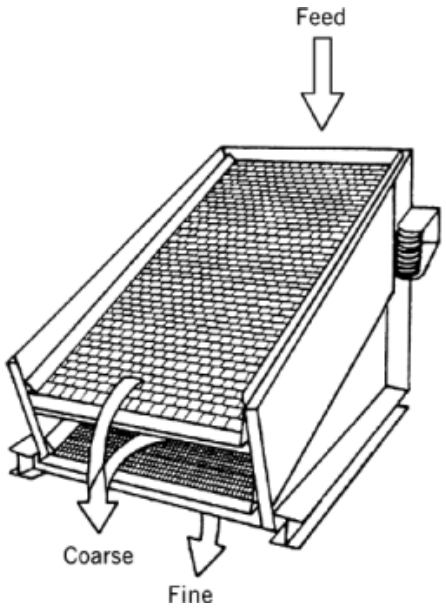

Fig. 3. Inclined vibrating screen.

much larger ones by draining or rinsing; dewatering (qv), ie, the removal of water from particles by draining; and prewetting, ie, the addition of water to the particles by spraying.

2.1. Equipment

Screening devices can have stationary or moving screen decks. Moving screen decks can be designed as rotating cylinders (trommels) or vibrating surfaces. By far, the most popular screen deck design for sizing is the inclined vibrating screen (Fig. 3). Components of vibrating screens are the vibrating frame, deck support frame, screening deck, motor/drive assembly, and feed box/distributor. Auxiliary components include conveyor belts, feed chutes, and dust collection systems. Vibration is produced on inclined screen decks by circular motion in a vertical plane of 3–12.5-mm amplitude at frequencies of 700–1000 cycles per minute. Newer high speed screening designs operate at 3600 cycles per minute. The vibration lifts the material, producing stratification. Stratification places the larger particles on top, and the smaller particles on the bottom, next to the apertures. This also helps push near-size particles through the apertures, reducing blinding. When the screen deck is used on an incline, the material cascades down the slope, introducing the probability that the particle either passes through the opening or over the screen surface. For horizontal screen decks, the motion must be capable of conveying the material without the assistance of gravity. Straight-line motion at an angle of approximately 45° to the horizontal produces a lifting component for stratification and a conveying component for probability of separation as the material passes across the horizontal screen surface. Industrial screens typically range from 2–7.5 m in length.

Some of the numerous factors influencing the passage of a particle through a screen opening are ratio between cross-section of particle and of opening, percentage of screen open area, angle of incidence of feed, efficiency of spread of feed over screen area, kinetic energy of particle approaching screen opening, moisture of feed, stickiness of particle and of aggregated particle, pressure of particles riding above those next to the screen deck, blinding of screen apertures, corrosion of deck material, electrostatic bunching, shape of particle, amount of near-size particles in the feed, rate of feed, thickness of the bed, tautness of deck, shape of screen

apertures, trajectory of particle imparted by amplitude and frequency of vibration, bulk density of material, and particle integrity (6). Because of the multitude of factors acting individually and interactively, no fundamental procedure based on first principles has been developed for sizing commercial screens. For example, increases in the quantity of near-size particles, ie, particles where the sizes lie between 0.5 and 1.5 times the aperture size, lead to more blinding, which in turn lead to a decrease in the percentage of open area, ie, the ratio of the aperture area to the screen deck area, which reduces the screening efficiency of the screen deck. Most manufacturers of vibrating inclined screens have developed variations on a design theme that involves estimating the design loading, defined as flow rate/screen area, and then dividing the design feed rate by the design loading to obtain the required deck area (7).

2.2. Design Loading

The design loading, or capacity, is estimated by starting from a basic loading for square screen cloth having the desired aperture size. The base loading decreases with decreasing aperture size, partially because the open area decreases. The base value assumes an optimal bed depth, deck slope (flow velocity), quantity of near-size material, free-flowing material, and screen open area. Thus, the base loading must be modified for material properties, equipment design, and operating conditions that differ from the standard ones. For example, there are modifying factors for bulk density, size distribution, and particle shape. The capacity decreases with increasing surface moisture for materials that become cohesive. When the problem is severe, wet screening, ie, water sprays mounted above the screen deck, should be considered. Wet screening increases the capacity, particularly for smaller aperture sizes. The base value is modified for percentage of open area, because capacity decreases directly with decreasing open area, and for aperture geometry, because capacity increases with rectangular apertures, but decreases with circular apertures, because the open area increases and blinding decreases. The base value also depends on whether the screen deck is on the top, middle, or bottom, because larger aperture decks are usually placed above smaller aperture ones in order to protect the smaller aperture deck from damage by large particles. The value is modified for deck slope and motion, ie, frequency, amplitude, and direction.

2.3. Deck Area

After the design loading has been estimated, the design feed rate is divided by the design loading to get the effective deck area. This value is usually increased by at least 10% to take into account blockage by hardware associated with the deck support frame. In order to convert the effective deck area into length and width dimensions, the deck width is calculated based on a standard bed depth. The width is selected such that the cross-sectional area of the volume of theoretical oversize leaving the screen deck has a height that is twice the aperture opening. Then the length is calculated by dividing the effective area by the width. Because the length determines the screen efficiency and the width determines capacity, the length should be at least twice the width.

Final screen selection is such that the length and width dimensions match off-the-shelf machines in order to keep costs down. Operating the installed screen at a feed rate greater or less than the design rate results in a less efficient screening operation, because bed depth varies with feed rate.

The top size of the feed to a screen deck should not be greater than two to four times the aperture size of the deck. Double- (see Fig. 3) or triple-deck screen arrangements are used, requiring a separate sizing for each deck. Then the final screen size is set by the largest deck.

Screen decks can be woven wire screens (including piano wire), perforated screen plate, or profile wire. Materials used range from ferrous and nonferrous alloys to rubber and plastic. Screen decks made of rubber or plastic flex reduce blinding, as does unique woven wire geometry. The addition of bouncing balls underneath the deck, or air sprays similar in concept to water sprays over the deck, are also used to reduce blinding.

Vibrating the screen deck, at very small amplitude but very high frequency, has also been used successfully to reduce blinding.

Data for dry screening on a 20-mm square aperture vibrating screen (8) indicate that the screen is relatively efficient, giving an apparent bypass value of 0.5%, sharpness index of 0.8, and a cut size of 20 mm. On the other hand, results (9) from a plant operating an 8 ft × 20 ft (2.4 m × 6.1 m) double-deck screen with 16 mm woven wire bottom screen deck gave an apparent bypass of 4%, sharpness index of 0.56, and a cut size of 17 mm. Data (10) for smaller apertures (0.5 mm) indicate that the cut size is smaller than the opening size, and higher sharpness indexes are only achieved using long screen lengths.

2.4. Slurries

Mixed results have been reported (11, 12) for screening slurries using small (100-μm) aperture vibrating screens. The ratio of cut size to aperture size decreases from 0.75 to 0.5 with increasing solids concentration. Because the sharpness index is directly proportional to the ratio, it decreases from 0.7 to 0.5. The apparent bypass value, which is essentially equal to the water split, increases with increasing feed rate and solids concentration. However, there are indications that the type of screen cloth used can affect these results when going from a square to an elongated rectangular aperture.

There is a family of stationary screens known as cross-flow screens, used mainly for dewatering or desliming, that have been applied to slurry sizing. The original member was the sieve bend where feed entering a curved sieve separates into two streams. The fines go through the slotted openings; the coarse stream follows the bend and exits off the end of the sieve. These screens are characterized by a slotted deck, usually made of stainless steel profile wire and set at an angle. The slurry flow is at right angles to the slots and, depending on the angle of inclination, the cut size value is one-half to two-thirds of the slot dimension. Hence, it is possible to size at 0.5 mm using a 1-mm slot, which should reduce blinding problems. However, as the slot dimension is reduced, the apparent bypass value increases, approaching 100% for a slot width of 40 μm. This can be substantially reduced (values approaching 5%) by vibrating the screen deck (13). Rapping, ie, using a large amplitude and low frequency, is not recommended. A typical sharpness index value is 0.5.

2.4.1. Probability Screens

Other approaches to reducing the blinding effect have included the development of so-called probability screens. Screen blinding led to the commercialization of a simple principle. The projected area of a rectangular aperture, normal to the horizontal, decreases as the angle of inclination of the screen deck containing the aperture increases. Thus, the probability of passage for a particle falling normal to the horizontal, which would normally pass through the aperture, decreases with an increasing angle of inclination. The probability of a particle lodging in the opening is minimal. The commercial sizer (Fig. 4**a**) consists of five superimposed screen decks, each with a slightly steeper slope and a smaller aperture than the one above. The screen apertures are no less than twice the desired separation size. Two out-of-balance motors transmit a linear vibration to each deck, and the resulting action fluidizes the feed so that the particles are presented essentially normal to the horizontal. This design can achieve separation sizes of 50 mm down to 100 μm at high capacity and minimal blinding compared to conventional screens.

Another screening design (Fig. 4**b**) developed to handle feed materials with extensive damp, clayey fines content is the rotating probability screen. The Ropro was developed by the National Coal Board in the U.K. (14) after it had rejected electrically heated decks, piano wires, loose rod decks, air sprays, bouncing balls, centrifugal screening, and flip-flop decks made from polyurethane that stretched, relaxed, and fluidized the material to be screened. The screen of the Ropro is created by fitting stainless steel rods to a vertical rotating shaft. The rods, radiating from the central hub, create a horizontal circular surface. The apertures between the radial elements of the screen progressively enlarge and the rods have no supporting members. These apertures are larger than the feed. If the deck is stationary, all the feed material passes through the apertures; if the

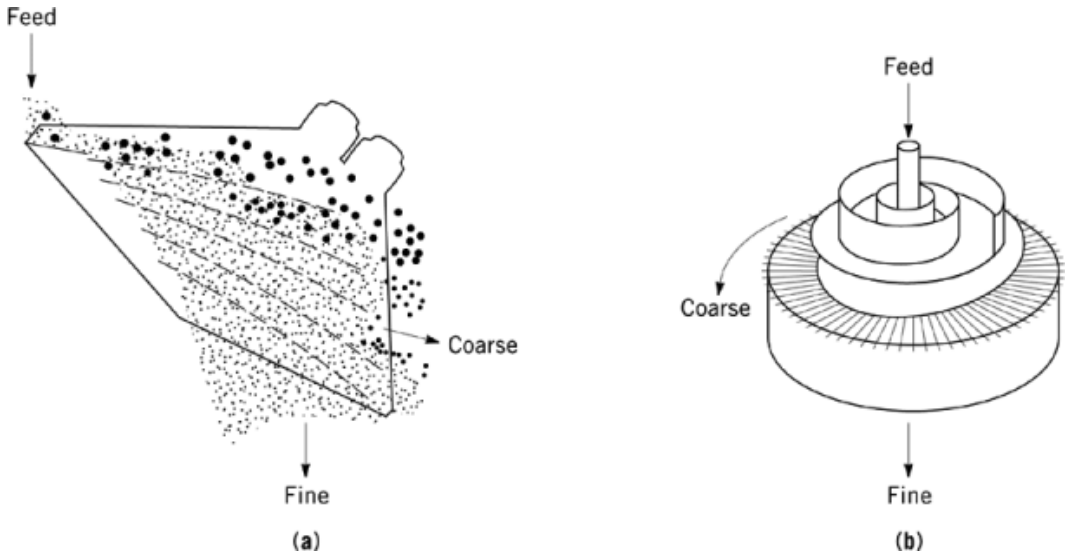

Fig. 4. Probability screens: (**a**) hi-prob sizer; (**b**) Ropro screen.

deck is rotated at high speeds, none of the feed material passes through the apertures. Thus, by controlling the speed of rotation, the screen size is regulated. Hence, the variable rotation speed creates a variable aperture screen. Although no blinding is claimed for this design, no screening efficiency data, particularly apparent bypass, have been reported. An upper deck, designed to scalp the feed to the lower deck, and a rotating table product-collecting system are available modifications.

3. Wet Classification

3.1. Settling-Pool Classifiers

The settling-pool group of fluid-dynamic separating devices (classifiers) (Fig. 5) consists of a rectangular tank having an inclined floor that creates a pool. Feed slurry is introduced at the side of the tank and the overflow of fine particles and water exits through an overflow weir and box arrangement. The coarse particles settle to the bottom and are discharged over the upper edge of the tank after being dragged up the inclined floor by some mechanism, such as intermittently operating rakes, continuously operating drag conveyors, or continuously operating spirals.

The length of time the particles stay in the pool determines the distance the particles settle in the pool. Thus, the feed entrance must be located so that the velocity of the pulp toward the weir, together with the distance, allows sufficient time for the fine particles to be carried out over the weir as the coarse particles settle out below. It is assumed that if a particle settles more than twice the overflow weir crest, it settles out as a coarse particle. The coarse particles are agitated and washed as they are conveyed up the inclined floor, thus reducing the amount of undersize particles carried out in the coarse stream. The pulp velocity, and hence time in the pool, can be varied by altering the weir geometry, the total volume flow, or the solids' concentration. All basically change the mean residence time, ie, the ratio of the mass of holdup material to the feed rate, by varying the mass of holdup material or the feed rate. However, some changes may force the pseudo-free settling conditions more toward hindered settling conditions, thus giving an unexpected result (see Sedimentation).

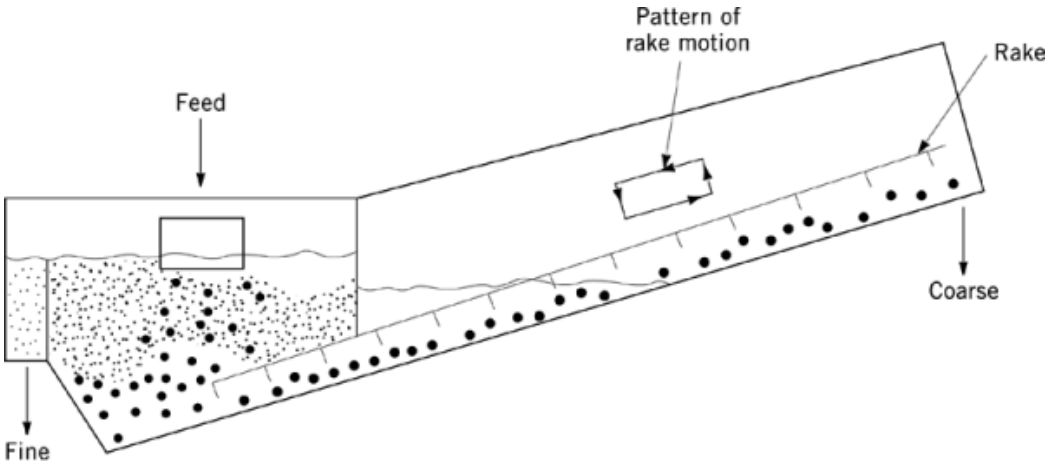

Fig. 5. Settling-pool classifier showing the rake and the pattern of rake motion. Incline is from 14–20° (25–35 cm/m).

The separation mechanism of a settling pool should be very straightforward (3). If a cylinder of slurry is shaken initially so that all the particles are uniformly distributed throughout the suspension, then all the particles immediately start to settle under the influence of gravity at rates determined by size, shape, density, and other factors. The upper half of the cylinder then contains particles given to the overflow whereas the lower half contains particles given to the underflow. A certain size of particles just settles from the top to the level at which the overflow and underflow are partitioned. The underflow contains all particles having settling rates greater than the certain size, particles having settling rates less than the certain size because those were near the level between the overflow and underflow, and particles of all settling rates which were originally distributed into the underflow. This last is called void-filling material and represents apparent bypassing for this type of classifier. Dividing the quantity of particles of each size remaining in the upper half by the quantity of particles of the same size in the initial slurry estimates p. The cut size and the apparent bypass values decrease with increasing settling time; the sharpness index increases, becoming essentially constant at about 0.6. The apparent bypass value is approximately equal to the water split, ie, the ratio of the amount of water in the lower half divided by the amount of water in the initial slurry. Superimposing turbulence upon this process produces the same pattern, except that the cut sizes are higher and the sharpness indexes lower after the same settling time.

Analysis of this type of classifier (15) suggests that the sharpness index is between 0.5 and 0.6, consistent with calculated results, because the degree of turbulence can be high in these devices (16). A DSF Dorr classifier ($1.8\ \text{m} \times 7\ \text{m}$), operating at 19 strokes per minute and having a weir depth of 100 cm and a slope of 19.4 cm/m, produced a cut size equal to 240 μm, a sharpness index of 0.5, and an apparent bypass of approximately 26% when the water split was 26% (15).

As the settling type of classifiers are used to produce finer size separations, the pool volume is increased. A settling-type classifier can be operated to produce cut sizes between 150 and 25 μm but having a corresponding decrease in the sharpness index from 0.5 to 0.2, apparently caused by the increased influence of turbulence (16). Also, the percentage of solids in the fine stream is reduced from 25 to 7% and the coarse stream percentage of water increases from 15 to 25%. This increases the apparent bypass percentage or void-filling material. In addition, because the maximum flow rate of the coarse stream is fixed for each device, the feed rate must be reduced, thereby reducing device capacity.

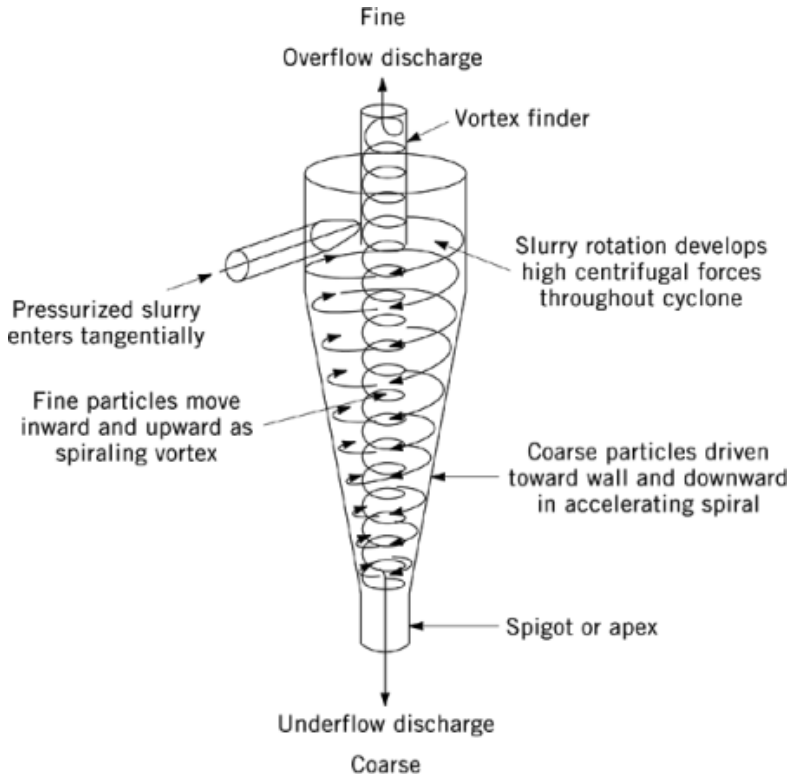

Fig. 6. Hydrocyclone classifier.

3.2. Hydrocyclones

Increasing the gravitational force by developing centrifugal force decreases the settling time of smaller particles. A centrifugal force can be imposed on particles by rotating the slurry of particles (see Separation, centrifugal separation). The classifying hydrocyclone (Fig. 6) is designed to rotate the slurry of particles by introducing it tangentially into a cylinder, thereby achieving essentially free vortex motion. A second, smaller-diameter (20–40% of the cylinder diameter) pipe, called the vortex finder, is placed through the exact center of the solid top of the cylinder, extending substantially below the feed inlet but above the bottom of the cylinder. The slurry that exits through the vortex finder is termed the overflow and contains the finer particles. Attached to the bottom of the cylinder is an inverted truncated cone section, the included angle of which ranges from 10–30° and is typically 15–17°. The slurry that exits through the cone section (apex) is termed the underflow and contains the coarser particles. The hydrocyclone is the most popular industrial wet classifier.

As the fluid rotates in the hydrocyclone, forming an air core in the center, there are three fluid velocities of interest: the tangential, the radial, and the axial (17). The tangential velocity, which is zero at the cyclone wall, increases immediately upon moving from the outer wall to the air core, reaching a maximum and then decreasing. There is a locus of constant tangential velocity. The radial velocity immediately increases from zero at the cyclone wall, but then, moving from the outer wall to the air core, decreases to zero. In the cone section, the axial velocity immediately drops from zero at the cyclone wall. A positive value indicates vertical movement. Then, moving from the outer wall to the air core, the axial velocity increases to positive values. Thus, the fluid motion is down the wall of the cyclone to the apex and up the air core through the vortex finder.

In the cylindrical section, the axial velocity goes negative again, approaching the vortex-finder wall. The fluid flow is then down the inner cyclone wall and the outer vortex-finder wall. There is a locus of zero axial velocity.

The diameter of the air core varies with the feed volumetric flow rate. If the rate is too low, there is no air core and all of the pulp leaves the cyclone as underflow; if the rate is too high, the air core expands, closing off the apex and forcing all of the pulp to leave the cyclone as overflow. Consequently there is a minimum and maximum volumetric feed rate. Because the pressure drop is proportional to the square of the volumetric feed rate, the minimum and maximum rates can be monitored by the pressure drop. The ratio of the maximum pressure drop to the minimum pressure drop should be less than 4, meaning the maximum to minimum volumetric feed rate should be less than 2.

A particle entering the cyclone finds a point where its velocity with respect to the fluid is equal to the radial velocity, and hence is at rest with respect to radial movement to or from the wall. Because the radial velocity changes with radius, the particle spirals down the cone section, following a path defined by the particle velocity with respect to the fluid equal to the radial velocity. This path is the equilibrium orbit for all particles of this mass and shape. Larger particles move toward the wall to find their equilibrium orbit, unless they reach the wall. Smaller particles move toward the air core to find their equilibrium orbit. Thus, a particle passes out in the overflow if its equilibrium orbit is to the interior of the locus of zero axial velocity; a particle passes out in the underflow if its equilibrium orbit is toward the outside of the locus. Particles having an equilibrium orbit on the locus define the equilibrium or d_{50} size. As the concentration of particles increases, this simple model (18) breaks down.

For a properly designed and operated cyclone, the sharpness index is constant, typically 0.6. The cut size and apparent bypass are a function of the cyclone geometry, the volumetric feed rate, the material relative density, the feed solids concentration, and the slurry rheology. The relationship for a standard cyclone geometry, where if D_c is the cylinder diameter in cm and inlet area = $0.05\ D_c^2$; vortex finder diameter = $0.35\ D_c$; $0.35\ D_c >$ apex diameter $> 0.1\ D_c$; and $20^\circ >$ included angle $> 10^\circ$ (19), is

$$d_{50},\ \mu\text{m} = 16.9\ \frac{D_c^{0.66}}{(\Delta P)^{0.28}\,(\rho_s - \rho_l)^{0.5}\left[1 - 1.9\ (V)\right]^{1.43}} \qquad (3)$$

where ΔP is the pressure drop in kPa, ρ_s is the relative density of the solid, ρ_l is the relative density of the liquid, and V is the volume fraction of the solids. This expression has no direct correction for slurry rheology. From this expression, it can be seen that the cut size d_{50} decreases with a decrease in the cylinder diameter and an increase in the pressure drop. Hence, in order to make fine separations, small-diameter cyclones operating at high pressure drops (200–350 kPa (29–51 psi)) should be used. Additionally, the cut size decreases with increasing solid relative density, but increases with increasing solids concentration. One manufacturer, Krebs Engineers (Menlo Park, California) offers cyclones in diameters of 2.5, 10, 15, 25, 38, 51, 66, 76, and 127 cm.

The apparent bypass can be estimated by assuming it is approximately equal to the water split, ie, the percentage of water in the feed that reports to the underflow. The water split has been found to follow a straight-line relationship with the inverse of the feed water rate for cyclones having diameters greater than 7.5 cm and standard geometries. However, for cyclones of smaller diameters, the apparent bypass appears to be much greater than the water split, and is typically proportional to the square root of the water split.

The solids concentration of the underflow must be monitored in order to prevent a roping condition from developing (20). A spiraling solid underflow stream is referred to as a rope discharge. The underflow stream should appear as a hollow cone spray having a 20–30° included angle. Typically, the maximum solids concentration of the feed stream is 30 vol %, the overflow (fine) stream is 15 vol %, and the underflow (coarse stream) is 55 vol %, which would produce a water split of 24%. In order to prevent roping, it is suggested that the underflow stream solids concentration by volume must be less than 49.3 plus one half of the overflow vol % solids.

Table 1. Characteristic Classification Parameters for Twin-Cone Classifier[ab]

	Vane setting, %		
Parameter	100	50	25
sharpness index	0.325	0.5	0.3
cut size, d_{50}, μm			
1700 m^3/h (1000 ft^3/min)	120	56	22
3400 m^3/h (2000 ft^3/min)	164	105	82
5100 m^3/h (3000 ft^3/min)	197	151	178
apparent bypass			
1700 m^3/h (1000 ft^3/min)	0.05	0.35	0.55
3400 m^3/h (2000 ft^3/min)	0.05	0.20	0.30
5100 m^3/h (3000 ft^3/min)	0.05	0.05	0.05

[a] Ref. 24.
[b] Diameter = 0.75 m.

Because the cut size decreases with cyclone diameter (d_{50} in μm $\cong 5\ D_c^{2/3}$ in cm) and because the capacity, l/s, also decreases with cyclone diameter ($l/s \cong 0.022\ D_c^2$), high classification capacity at low cut sizes can only be achieved by feeding many cyclones of the same diameter. The manifolding of cyclones for parallel processing becomes very important. Each cyclone must be fed at the same pressure using the same amount of solids having the same particle size distribution, therefore radial manifolding is usually recommended in order to achieve uniform distribution of the feed; in-line manifolding usually gives poor distribution.

3.3. Centrifuges

Solid-bowl centrifuges have been proposed as an alternative classifying device to hydrocyclones for cut sizes below 10 μm. The results appear to be mixed (21). In one application, where the cut size was 6.5 μm and the sharpness index 0.7, there was essentially no apparent bypass. However, in other applications operating at higher feed concentrations, the cut size ranged from 5–8 μm, but the sharpness index was between 0.3–0.5 and the apparent bypass between 10–30% or higher (22). Smaller cut sizes have also been reported (23).

4. Dry Classification

Pneumatic classification can be partitioned conveniently into coarse, ie, fine products above 95% < 100 μm; intermediate, ie, fine products ranging between 95% < 100 and 30 μm; and fine, ie, fine products below 95% < 30 μm. Pneumatic classification, like hydraulic classification, balances the force of gravity with drag forces (counter flow) in order to bring about a separation.

The vane classifier (Fig. 7) is an example of a free-vortex counterflow classifier. The solids to be classified enter the outer cone dispersed and entrained in a gas stream. A cyclone flow pattern is imparted on the feed stream before it passes through the adjustable vanes into the inner cone. As the vanes are closed down, an increase in the centrifugal motion causes more of the larger particles to strike the inner wall of the inner cone and drop out. The finer particles remain in the gas stream, exiting through the centrally located exit conduit. For a pilot-scale twin-cone classifier, the sharpness index was constant for a set vane position (24). As the vanes were adjusted from 100 (an expansion classifier) to 50 to 25% (a pneumatic cyclone) open, the sharpness index increased but then decreased at the 25% vane setting (Table 1). Increasing the air rate, thereby also increasing the feed rate, caused a decrease in the apparent bypass, but an increase in the cut size for each vane setting.

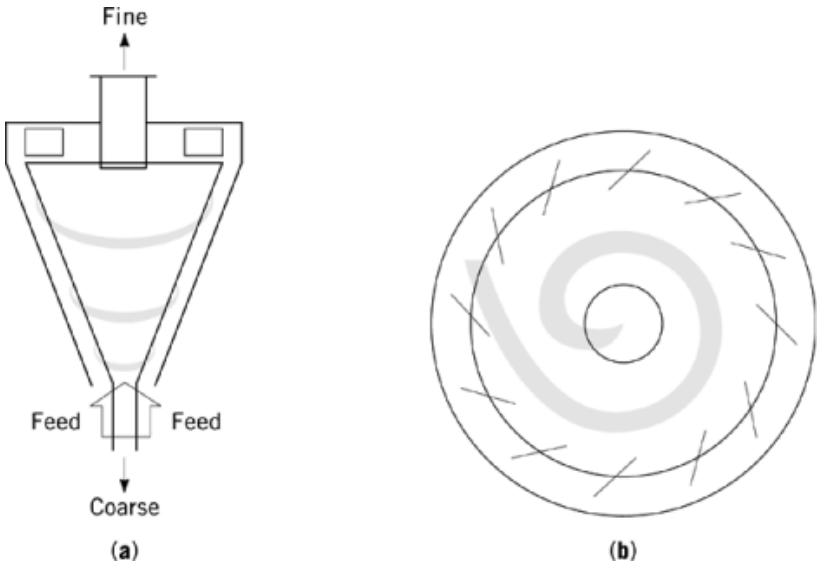

Fig. 7. Vane classifier where ($_{\square}$) represents particle flow: (**a**) side view and (**b**) cross-sectional view showing the vanes.

The free-vortex principle has been extended to fine classification. A built-in fan in the second chamber of the two-chamber Alpine Mikroplex Spiral classifier draws the classifying air into the classifier chamber while the feed is metered in separately. Adjustable vanes control the angle of air-flow approach to the center of the chamber where the fines flow out. The coarse particles are thrown to the outside and removed mechanically from the casing of the chamber. The sharpness index varies between 0.65 and 0.7, decreasing as the feed rate and hence solids loading increases. The cut sizes range between 10 and 80 μm, depending on the vane setting and the fan speed. No apparent bypass has been reported, but it is appropriate to assume about 5%. This value increases as the feed rate increases.

An alternative design is that of the forced vortex in which the vanes are rotated. The Mikropul Acucut classifier (Fig. 8) draws air in via a vacuum pump. The fines pass through the rotor, discharging out the center. The coarse particles are removed at the outer periphery. The sharpness index varies between 0.6 and 0.8, decreasing as the solids loading increases. The cut sizes range between 2–30 μm, depending on the rpm of the rotor. The d_{50} is inversely proportional to the rpm$^{1.4}$. Whereas no apparent bypass has been reported, values of approximately 5% have been measured. The forced vortex is less sensitive to solids loading than the free vortex.

The use of a rotor has been the cornerstone of the mechanical air classifier. Rotor design has changed from blades to the multivane or post design (Fig. 9). In this device, the feed material is dispersed in the airstream drawn through the rotor. Whether or not a particle exits in the central fine particle discharge depends on the force balance between the drag force of the particle being conveyed and the centrifugal force created by the rotor against it. The cut size is proportional to the air flow rate raised to a power between 1 and 2 and inversely proportional to the rpm of the rotor and the square root of the relative density of the feed material. Values range between 5 and 150 μm. Operating sharpness indexes can reach 0.75.

Data for a pilot device (25) using a blade rotor design are given in Table 2. The sharpness index was a constant 0.6. There are several responses common to classifiers employing rotors. Increasing the feed rate without any other changes reduces the d_{50} value, the efficiency of the separation, and the yield. The data in Table 2 demonstrate a consistent pattern, in all cases, of the d_{50} value decreasing to a minimum with increasing feed rate. Moreover, the efficiency of the classification is reduced with increasing feed rate because the apparent

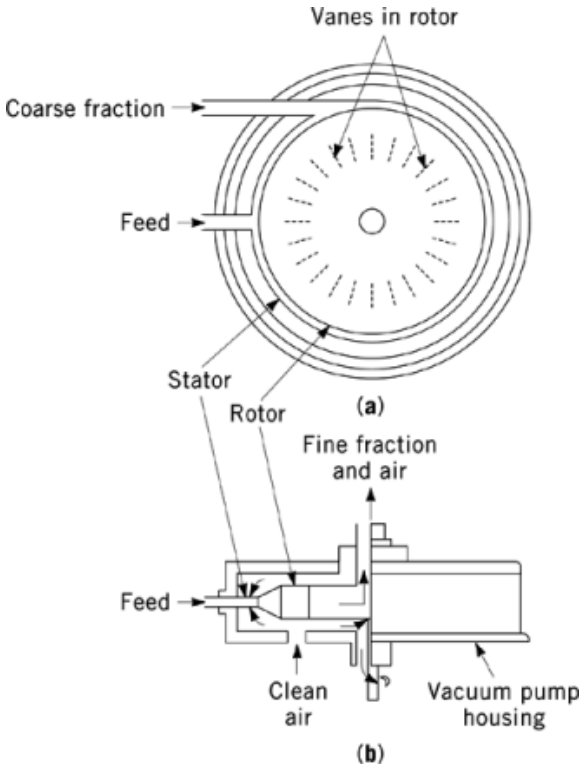

Fig. 8. Views of a Mikropul Acucut classifier: (**a**) cross section and (**b**) side view.

bypass value increases. The yield also decreases with increasing feed rate, because the increased quantity of feed, when going from a relative feed rate of 4 to 7, is merely bypassing to the coarse stream. Assuming the air flow rate to be proportional to fan speed, then the data for a rotor rpm of 1000 give d_{50} proportional to the air-flow rate to the 1.2 power. The 800 and 1400 rotor rpm data show that the d_{50} value is inversely proportional to the rotor rpm. Industrial versions of this separator come in sizes up to 10 m in diameter.

A recirculation design (Fig. 10) returns the gas to the classifier through the fan after the fine particles are removed from the gas stream. Such an arrangement requires an excellent solid/gas separator; otherwise the classification becomes less efficient. A perfect solid/gas separator would be a device having $a = 1$. If the recirculated gas is entered through a secondary coarse stream classification section, then the classification is not less efficient unless the secondary classification is very inefficient.

It is quite common in the designs for fine classification to recontact the coarse stream transversely or in counterflow with air before discharging it (see Fig. 9). This removes dry fine particles not removed in the primary classification. That is, these particles are swept back into the feed and given another chance to exit with the fine particles. Such an arrangement increases the overall sharpness index and reduces the overall apparent bypass. Another variation is to reenter the air from the solid/gas separation of the coarse stream.

The Matsuzaka Elbow-Jet classifier (Fig. 11) is based on a transverse flow principle (26). The stream of feed particles are accelerated to minimize the effect of gravity, and introduced into an air jet at right angles. The particles are fanned out in the classification zone with the trajectories for particles of the same hydrodynamic behavior, ie, size and shape, being the same. Classification is achieved by mounting one or more cutters in the

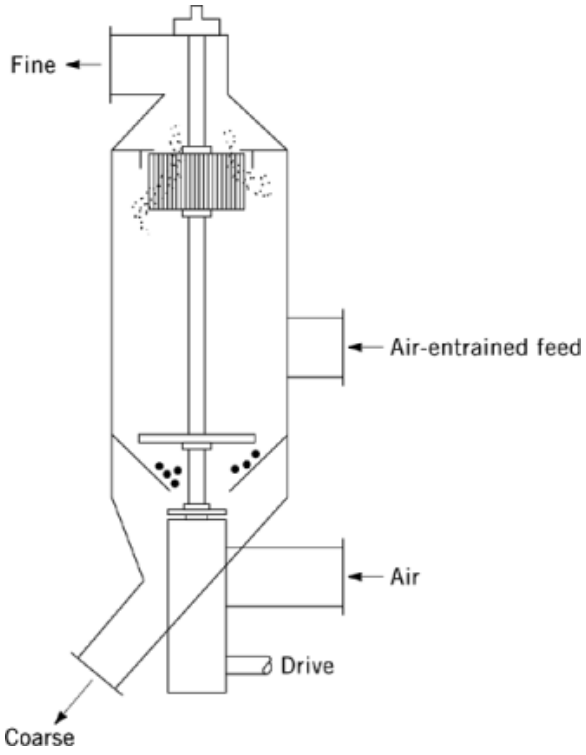

Fig. 9. Tank through-flow classifier.

classification zone, thus dividing the feed into two or more fractions. A stream of fine particles of less than 5 μm can be produced in this manner.

The concept of stage classification in order to improve the classification has been used in both hydraulic and pneumatic classifier installations (27). Different arrangements result in a reduction in the global apparent bypass, an increase in the global sharpness index, or a decrease in the global cut size, compared to the individual units. The underflow/overflow recirculating arrangement (see Fig. 12) can achieve all three global improvements: the sharpness index increases by over 10%; the cut size decreases by 15%; and the apparent bypass decreases by 50%.

5. Health and Safety Factors

The pneumatic classification system should be designed to handle hazardous dust (28). A hazardous dust is one which, when finely divided and suspended in air in the proper concentration, burns, produces violent explosions, or is sufficiently toxic to be injurious to personnel health (see Air pollution control methods; Powders, handling). At the least, almost any dust can be irritating to personnel because of inhalation or skin or eye contact. Fully oxidized and hydrated materials are generally considered safe.

Dust explosions usually occur in pairs. The first explosion involves dust already in suspension. This jars dust from beams, ledges, etc, creating a second cloud to which the explosion propagates, resulting in a secondary explosion. Dust clouds have been ignited by open flames, electric sparks, hot filaments of light bulbs, friction sparks, hot surfaces, static sparks, spontaneous heating, welding and cutting torches, and other

Table 2. Characteristic Classification Parameters for a Mechanical Air Separator[ab]

Fan, rpm	Rotor, rpm	Relative feed rate	d_{50}, μm	Apparent bypass	Yield
1400	600	1	62.5	0.05	0.57
1400	600	4	40	0.50	0.20
1400	600	7	40	0.75	0.11
1400	1000	1	32.5	0.10	0.33
1400	1000	4	30	0.75	0.09
1400	1000	7	30	0.80	0.07
1850	800	1	60	0.05	0.55
1850	800	4	40	0.30	0.29
1850	800	7	40	0.40	0.23
1850	1000	1	45	0.05	0.46
1850	1000	4	35	0.30	0.25
1850	1000	7	35	0.50	0.18
1850	1400	1	35	0.05	0.40
1850	1400	4	30	0.40	0.19
1850	1400	7	30	0.60	0.13

[a] Ref. 25.
[b] Diameter = 1.2 m.

common sources of heat for ignition. Dust-ignition temperatures, for the most part, are 300–600°C. A large majority of the reported minimum spark energies for ignition of dust are <100 mJ (<24 mcal), which is much lower than the energies found in stray electric currents and static electricity discharges. The finer the dust, the greater the concern.

Dust explosions can be minimized by elimination of any leg of the basic fire triangle, ie, source of ignition, oxygen, and fuel. Elimination of the source of ignition and oxygen (<10 wt%) are possible. Dust must be controlled by utilizing air-to-solid ratios throughout the system that keep dust concentrations below a minimum level or above a maximum level. Most organic materials, including plastics, have a minimum explosive concentration of 15–300 g/m^3, and that of metals can approach 500 g/m^3.

The equipment in which the dust is handled or stored should be designed to contain the pressure resulting from an internal explosion. Most dusts show maximum pressures of ca 345–700 kPa (50–100 psi); however, the rate of pressure rise changes from ca 700 to 70,000 kPa/s (100–10,000 psi/s). Equipment-containment design can be coupled with explosive-venting design for the equipment and the building.

Sometimes conveying (qv) velocities, typically 20–25 m/s, exceed the flame-propagation rate as determined by tests. Moreover, velocities vary throughout the system. If the flame-propagation rate exceeds the conveying velocities, consideration must be given to the isolation of parts of the system by choking, ie, the use of rotary values, screen conveyors, bins, etc.

Proper ventilation and housekeeping minimizes secondary explosions. Dust collectors of the dry type should be located outside the building, and provided with conduction bags and adequate explosion venting to a safe location.

6. Prediction of Size Separation

Most corrected characteristic separation curves (27) fit the following logistic function:

$$c\,(x_i;\ \kappa,\ d_{50}) = 1/\left(1 + e^{-Y_i}\right) \qquad (4)$$

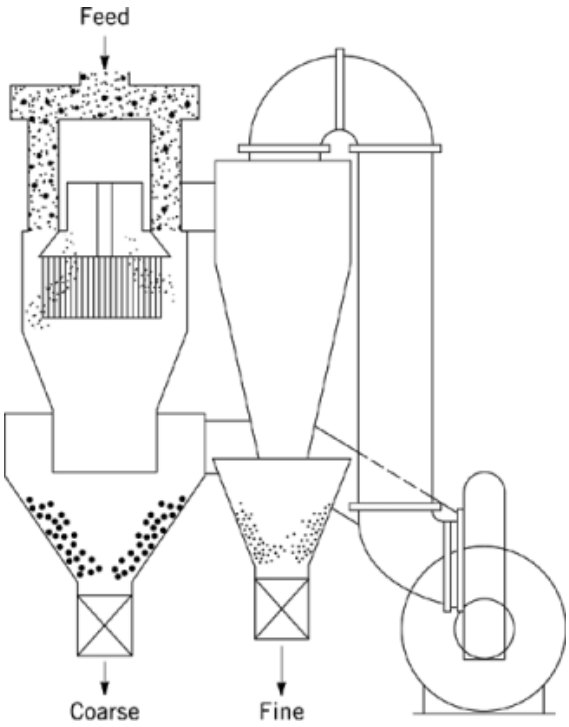

Fig. 10. Recirculating mechanical air separator.

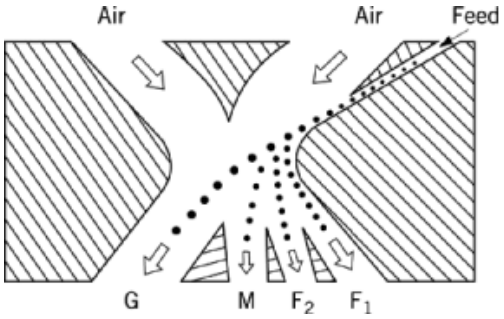

Fig. 11. Cross-sectional schematic of a Matsuzaka Elbow-Jet classifier where $_{F_1=\text{ultrafine}}$ particles, $_{F_2=\text{fine}}$ particles, $_{M=\text{medium}}$ particles, and $_{G=\text{coarse}}$ particles.

where Y_i equals $1.0986\,(1-z_i)\,(1+\kappa)/(1-\kappa)$ or $2.1972\,\ln[z_i]/\ln\,[\kappa]$ and z_i equals x_i/d_{50}, where x_i is the upper size of the narrow size interval, typically $x_i/x_{i+1} \leq \sqrt{2}$, hence x_1 is the maximum size. Thus, if the operating sharpness index and cut size are known for a separating device, the size distribution of the fine stream can be predicted. For example, if a feed having the size distribution given in columns 2 and 3 in Table 3 is to be classified, using a device with a sharpness index of 0.6 and a cut size of 100 μm, then using Y_i equal to $2.1972\,\ln[z_i]/\ln[\kappa]$, the corrected values (column 4) can be calculated. There must be a sufficient number of size intervals such that at least one value equals zero and one equals one. Next, the fine stream mass values (column 5) are calculated as the product of the column 3 element times the column 4 element. The fine stream interval values (column 6) are calculated by dividing the column 5 elements by the sum of column 5. Predictions,

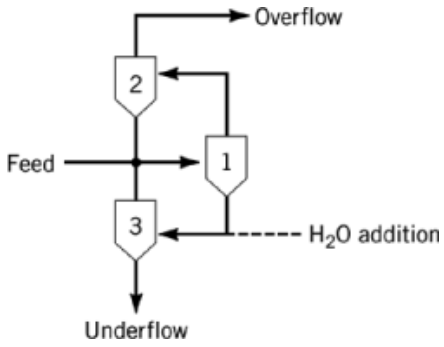

Fig. 12. A triple-stage classifier arrangement.

Table 3. Size-Separation Predictions[a]

	Feed			Fine	
z_i[b]	Cumulative	Interval	$c(z_i; \kappa)$	Mass[c]	Interval[d]
10.0	99.9	0.15	0.00	0.00	0.0
7.1	99.75	1.25	0.00	0.00	0.0
5.1	98.5	4.5	0.00	0.00	0.0
3.55	94.0	11.5	0.00	0.00	0.0
2.5	82.5	16.0	0.02	0.32	0.9
1.8	66.5	16.5	0.07	.15	3.3
1.25	50.0	15.0	0.28	4.20	11.9
0.9	35.0	11.0	0.61	6.71	19.0
0.63	24.0	8.0	0.88	7.04	20.0
0.45	16.0	5.5	0.97	5.34	15.2
0.32	10.5	5.5	0.99	5.45	15.5
0.20	5.0	5.0	1.00	5.00	14.2
Sum				*35.21*	

[a] Using corrected probability of reporting to the fine stream values.
[b] $z_i = x_i/d_{50}$. See eq. 4.
[c] Product of feed interval and $c(z_i, \kappa)$.
[d] Fine mass value divided by summation of masses $= 35.21 \times 100$.

using a spread sheet, can be used to determine the cut size required to produce the desired product size distribution.

The yield is the sum of column 5 multiplied by $(1 - a)$. Thus, if the operating apparent bypass of the classifier is 0.3, then the yield is 24.65% or 0.2465. The coarse mass values can be calculated by subtracting the fine mass values multiplied by $(1 - a)$ from the feed interval values. The coarse interval values are then calculated by dividing the coarse mass values by the sum of the coarse mass values.

Table 4. Costing Parameters for Size Separators[a]

Parameter	X	a	b
	Vibrating screens		
single deck, m^3	0.5–45	9,591.44	0.4069
double deck, m^3	0.5–45	10,918.50	0.4256
triple deck, m^3	1.5–45	11,249.90	0.4908
	Spiral classifiers		
simplex, cm	60–125	481.86	1.008
	125–215	4.24	1.986
duplex, cm	60–130	611.65	1.043
	130–200	17.22	1.776
	Wet cyclones		
D_c, cm	2.5–35	214.74	0.7582
D_c, cm	35–130	20.01	1.430

[a] See eq. 5.

7. Economic Aspects

The cost of size separation devices varies according to type of separator and the sizing of the components. However, the approximate cost of many of the size-separation devices follow the form,

$$\$ = aX^b \qquad (5)$$

where X is a suitable parameter and a and b are an appropriate coefficient and exponent, respectively. The cost, in U.S. dollars, can be updated by cost index ratio adjustment because the dollars are for a Marshall and Swift mining and milling industry index of 1000 (29).

For vibrating screens, the suitable parameter X is the screen deck area multiplied by the length in m^3. Cost includes drive- and feed-boxes, and excludes motor, starter, and screen cloth. For spiral classifiers, the suitable parameter X for costing is the spiral diameter, in cm. Cost includes the motor. For hydrocyclones, the suitable parameter X for costing is the cyclone diameter, D_c, in cm. Cost includes fittings and combination urethane–ceramic liners. The appropriate values of X and the coefficients are given in Table 4.

BIBLIOGRAPHY

"Size Separation" in *ECT* 1st ed., Vol. 12, pp. 520–523, by W. A. Lutz, F. L. Bosqui, and A. D. Camp, The Dorr Co.; in *ECT* 2nd ed., Vol. 18, pp. 366–399, by F. L. Bosqui, Consultant; in *ECT* 3rd ed., Suppl. Vol., pp. 846–871, by P. Luckie, The Pennsylvania State University.

Cited Publications

1. T. Allen, *Particle Size Measurement*, 4th ed., Chapman & Hall, New York, 1990.
2. A. M. Gaudin, *Principles of Mineral Dressing*, 1st ed., McGraw-Hill Book Co., Inc., New York, 1967.
3. L. G. Austin, C. H. Lee, F. Concha, and P. T. Luckie, *Min. Met. Process.*, **9**, 161–168 (1992).
4. Equipment Testing Procedure Committee, *Particle Size Classifiers, A Guide To Performance Evaluation*, 2nd ed., AIChE, New York, 1993.
5. R. T. Hukki, in M. J. Jones, ed., *Proceedings of the 10th IMPC*, IMM, London, 1974, p. 240.
6. E. J. Pryor, *Mineral Processing*, Elsevier, New York, 1965.

7. J. P. Nichols, in Mular and Jergenson, eds., *Design and Installation of Comminution Circuits*, AIME, New York, 1982, Chapt. 27.
8. R. J. Batterham, K. R. Weller, T. E. Norgate, and C. J. Birkett, *International Particle Technology Symposium Proceedings*, Amsterdam, the Netherlands, 1980.
9. A. L. Mular, personal communication, 1990.
10. T. Brereton and K. R. Dymott, in Ref. 5, 181–194.
11. J. Slechta, I. J. Taggart, B. A. Firth, and E. Gallagher, *An Evaluation of a Novel Vibrating Fine Screen*, unpublished report, 1981.
12. R. S. C. Rogers, *Powder Technol.* **31**(1), 135 (1982).
13. W. Benson and C. Burgess, *Proceedings 5th ICPC*, Washington, D.C., 1966, 297–311.
14. D. Jenkinson, *Min. Cong. J.* **68**, 29 (July, 1982).
15. E. J. Roberts and E. B. Fitch, *Trans. SME*, 1113 (1956).
16. H. Schubert and T. Neese, in Ref. 5, 213–239.
17. D. F. Kelsall, *Trans. Inst. Chem. Eng. (London)* **30**, 87 (1952).
18. D. Bradley, *The Hydrocyclone*, Pergamon Press, New York, 1965.
19. R. A. Arterburn, in A. L. Mular and G. D. Jergenson, eds., *Design and Installation of Comminution Circuits*, AIME, New York, 1982, Chapt. 32.
20. A. L. Mular and N. A. Jull, in A. L. Mular and R. B. Bhappu, eds., *Mineral Processing Plant Design*, 2nd ed., AIME, New York, 1982, Chapt. 17.
21. P. Scheffler and P. Zahr, *World Mining* **33**(3), 50 (1980).
22. D. Timmermanne and K. Schobert, in J. A. Herbst, ed., *Proceedings 19th IMPC*, San Francisco, 1995, 65–68.
23. H. W. Hennicke and J. Steun, *Mater. Sci. Eng.*, **A109**, 3–7 (1989).
24. Committee on Comminution and Energy Consumption, *National Academy of Sciences Report No. 364*, 1981.
25. L. G. Austin and P. T. Luckie, *ZKG* **29**, 452 (Oct. 1976).
26. H. Rumpf and K. Leschonski, *Chem. Ing. Tech.* **39**, 1231 (1967).
27. P. T. Luckie, in K. V. S. Sastry and M. C. Fuerstenau, eds., *Challenges in Mineral Processing*, SME, Colorado, 1989, Chapt. 13.
28. Technical data, H. Boyd & Associates, Tequesta, Fla., 1981.
29. "Economic Indicators", *Chem. Eng.* monthly.

PETER LUCKIE
Penn State University

Related Articles

Separation, Centrifugal Separation; Separation, Magnetic Separation